

# Transport Studies of AlGa<sub>N</sub>/Ga<sub>N</sub> High Electron Mobility Transistor Structures

Sneha P. Chheda

Department of Microelectronics Research Group, University of Western Australia, Australia  
[snehapchheda@gmail.com](mailto:snehapchheda@gmail.com)

## Abstract

The Gallium Nitride High Electron Mobility Transistor (HEMT) is showing great promise towards development of the military radar systems, communication systems, high voltage and power systems and electronic surveillance systems. In this paper, the transport properties of AlGa<sub>N</sub>/Ga<sub>N</sub> HEMT structures i.e. Two dimensional electron gas (2DEG) sheet charge density and 2DEG mobility at room temperature (300K) are studied with the results obtained from theoretical 1D Poisson simulation and Hall effect for used in bio-sensing applications.

**Keywords:** AlGa<sub>N</sub>/Ga<sub>N</sub> HEMT, Two-dimensional electron gas (2DEG), Sheet charge density, Mobility, 1D Poisson simulation, Hall Effect

## 1. Introduction

Despite very extensive applications in just about every sphere of life, electronic devices from Si, GaAs and their alloys are intolerant of elevated temperatures and caustic environments.

Property	Si	GaAs	GaP	3C SiC (6H SiC)	Diamond	GaN
Band gap (eV) at 300 K	1.1	1.4	2.3	2.2 (2.9)	5.5	3.39
Maximum operating temperature (K)	600?	760?	1250?	1200 (1580)	1400(?)	
Melting point (K)	1690	1510	1740	Sublimes >2100	Phase change	
Physical stability	Good	Fair	Fair	Excellent	Very good	Good
Electron mobility RT, cm <sup>2</sup> /V s	1400	8500	350	1000 (600)	2200	900
Hole mobility RT, cm <sup>2</sup> /V s	600	400	100	40	1600	150?
Breakdown voltage E <sub>b</sub> , 10 <sup>5</sup> V/cm	0.3	0.4	-	4	10	5?
Thermal conductivity c <sub>T</sub> , W/cm	1.5	0.5	0.8	5	20	1.3
Sat. C. etc. drift vel. v(sat), 10 <sup>7</sup> cm/s	1	2	-	2	2.7	2.7
Dielectric const. K	11.8	12.8	11.1	9.7	5.5	9

Table 1: - Comparison of semiconductor properties for high-temperature electronics [2]

Group III nitrides possess several remarkable physical properties that make them particularly attract for reliable solid state applications. The wide bandgap materials possess low dielectric constants with high thermal conductivity pathways. They exhibit fairly high bond strengths and very high melting temperatures. The large bond strength inhibits dislocation motion and improves reliability in comparison to other II-VI and III-V materials. The nitrides are also resistant to chemical etching and allow GaN-based devices to be operated in harsh environments. The bandgaps of III-V nitrides are wide and direct, being 0.65eV for InN [1] and 6.2eV for AlN [1]. GaN itself possess a large bandgap of 3.4eV [1], a very high breakdown field ( $5 \times 10^6$  Vcm<sup>-1</sup>) [2] and an extremely high peak ( $3.1 \times 10^7$  cm s<sup>-1</sup>) [1] and saturation velocity ( $2.7 \times 10^7$  cm s<sup>-1</sup>) [2]. AlN can be alloyed with GaN, allowing a tuneable bandgap and hence a variable emission or absorption wavelength. Due to strong chemical bonds in the semiconductor crystal, GaN based devices are also promising for high temperature operation and applications under radiation exposure.

## Gallium Nitride Based Transistor

One GaN based devices that is expected to have a promising future is the transistor. GaN has been used as Metal-Semiconductor Field Effect Transistor (MESFET) and Heterojunction Field Effect Transistor (HFET), GaN Metal Insulator Field Effect Transistors (MISFETs) and current controlled devices such as Heterojunction Bipolar Transistor (HBT). These devices were designed and investigated as possible superior alternatives to current solid-state electronics such as Silicon (Si) and Gallium Arsenide (GaAs) based transistors as well as vacuum tube devices. GaN based transistors have high current gain cut-off frequency, f<sub>T</sub>, because of its high saturation velocity. The high heat tolerance capability allows GaN based devices to withstand temperatures as high as 500°C. Silicon based transistors become unreliable at 150°C and fail altogether at 200°C while use of GaAs based devices is restricted at high temperatures [6]. GaN semiconductor crystal has high bond strengths (approx. 2.2eV/bond) [4]. So, they are able to show high thermal and chemical stability, which is suitable for applications in harsh temperature environments. The AlGa<sub>N</sub> barrier layer is of the order of 200 to 300 Å [1] in the basic DC fabricated HFET. If this barrier thickness is scaled

down to 100 A°, the characteristics of the device can be improved. The high values of sheet carrier concentration  $n_s$  of the order of  $4 \times 10^{13} \text{ cm}^{-2}$  and sheet concentration-mobility products of approximately  $4 \times 10^{16} \text{ 1/Vs}$  were reported by Gaska et al. [5]. Presently, GaN and AlGaN layers are grown on sapphire or Silicon Carbide (SiC) substrates, which have lattice mismatches of 13.8% and 3.4% respectively [7].

### Mobility

The mobility of the carriers in AlGaN/GaN heterostructures found to vary inversely with the bandgap of the material and the temperature. It has been reported that the mobility of the charge carriers i.e. electrons is highest at low temperature but it starts degrading as the temperature becomes higher and higher. This all happens due to the various scattering mechanisms dominating at different temperatures. The mobility of the two-dimensional electron gases in AlGaN/GaN heterostructures is good with mobility values as high as  $5000 \text{ cm}^2/\text{Vs}$  have been measured [8]. The dependence of the mobility on bandgap can be explained by the increase effective mass,  $m^*$  of the electron [9].

### 2. Problem Definition

To study the transport properties of AlGaN/GaN HEMT heterostructures with different aluminum concentration obtained from the University of California, Santa Barbara. Specifically, it involves extracting the carrier mobility and concentration of the Heterostructures. The device consists of undoped AlGaN and GaN layers, grown on a sapphire substrate along the c-plane by metal-organic chemical vapour deposition (MOCVD).

It involves finding the sheet charge density and hall mobility of two-dimensional electron gas with the help of 1D Poisson Program developed by Gregory Snider [3], which gives, simulated sheet charge densities at the interface and Hall Effect at 1T magnetic field, which allows calculating sheet charge density as well as mobility, and compares the end results.

### 3. Experimental Methods

#### 3.1 1D Poisson Simulation

1D Poisson is a program for calculating energy band diagrams for semiconductor structures. It solves the one-dimensional Poisson and Schrodinger equations self-consistently. The program used in the simulation is attached in the appendices [3].

#### 3.2 Hall Effect

The Hall Effect describes the behaviour of the free carriers in a semiconductor, when an electric and magnetic field

are applied simultaneously. Figure 4.1 shows a semiconductor bar with a rectangular cross section and length  $L$ . A voltage  $V_x$  is applied between the two contacts as shown in figure resulting in a field along the x-direction. The magnetic field is applied in the z-direction.

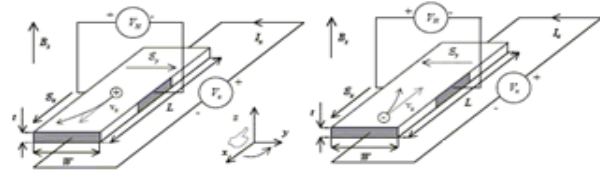


Figure 4.1: - Hall Effect with (a) Holes and (b) Electrons [10].

### 3.3 Calculations

The connections for Hall voltage measurements are shown in Figure. Here, current is applied and voltage is measured across the diagonal of the sample. Here, eight measurements are taken, both with positive and negative current, and positive and negative magnetic flux respectively. These voltages are designated V1 through V8.

The summary for Hall Voltage Measurements is as shown in the table below [modified from 11]

Voltage Designation	Flux	Current Applied Between	Voltage Measured Between
V <sub>1</sub>	+B	1-3	4-2
V <sub>2</sub>	+B	3-1	4-2
V <sub>3</sub>	+B	2-4	1-3
V <sub>4</sub>	+B	4-2	1-3
V <sub>5</sub>	-B	1-3	4-2
V <sub>6</sub>	-B	3-1	4-2
V <sub>7</sub>	-B	2-4	1-3
V <sub>8</sub>	-B	4-2	1-3

#### 3.3.1 Resistivity Calculations

After measuring voltages and current through the sample, the resistivity can be calculated as follows. Two values of resistivity  $\rho_A$  and  $\rho_B$ , are computed as follows:

$$\rho_A = \frac{1.133 \cdot I \cdot t_s \cdot (V_2 + V_4 - V_1 - V_3)}{I} \quad (1)$$

$$\rho_B = \frac{1.133 f_B * t_s * (V_6 + V_8 - V_5 - V_7)}{I} \quad (2)$$

Where:  $\rho_A$  and  $\rho_B$  are resistivity in ohm-cm,  $t_s$  is the sample thickness in cm,  $V_1$ - $V_8$  represent the voltages measured,  $I$  is the current through the sample in amperes and  $f_A$  and  $f_B$  are the geometrical factors based on sample symmetry and are related to the two resistance ratios  $Q_A$  and  $Q_B$  as shown below.  $Q_A$  and  $Q_B$  can be calculated using the measured voltages from table as follows:

### 3.3.2 Hall Coefficient Calculations

After measuring the voltages, the two Hall coefficients,  $R_{HC}$  and  $R_{HD}$  are calculated as follows:

$$R_{HC} = \frac{2.5 * 10^{-8} * t_s * (V_2 - V_1 + V_5 - V_6)}{BI} \quad (3)$$

$$R_{HD} = \frac{2.5 * 10^{-8} * t_s * (V_4 - V_3 + V_7 - V_8)}{BI} \quad (4)$$

Where:  $R_{HC}$  and  $R_{HD}$  are Hall coefficients in  $\text{cm}^3/\text{C}$ ,  $t_s$  is the sample thickness in cm,  $B$  is the magnetic flux in gauss,  $I$  is the current measured and  $V_1$ - $V_8$  are the voltages measured.

After calculating  $R_{HC}$  and  $R_{HD}$ , the average Hall Coefficient,  $R_{Havg}$ , can be determined as follows:

$$R_{Havg} = \frac{(R_{HC} + R_{HD})}{2} \quad (5)$$

### 3.3.3 Hall mobility Calculations

After measuring the Hall coefficient and resistivity, the Hall mobility can be calculated as follows:

$$\mu = \frac{R_{Havg}}{\rho_{avg}} \quad (6)$$

Where:  $\mu$  is the Hall mobility in  $\text{cm}^2/\text{V-s}$ ,  $R_{Havg}$  is the average Hall coefficient in  $\text{cm}^3/\text{C}$ ,  $\rho_{avg}$  is the average resistivity in ohm-cm.

### 3.3.4 2DEG sheet charge density

$$n_s = \frac{1}{R_{Havg} e} \quad (7)$$

Where:  $n_s$  is the 2DEG sheet charge density in  $\text{cm}^{-2}$ ,  $R_{Havg}$  is the Hall coefficient in  $\text{cm}^3/\text{C}$ ,  $e$  = electron charge in  $\text{C}$

## 4. Results and Discussions

### 4.1 Dependence of 2DEG sheet charge density on aluminium content with Hall measurements

The graph of 2DEG sheet charge density as a function of aluminium content of the AlGaIn layer for the set of measurements where  $x_{Al} = 0.15, 0.23, 0.29, 0.35$  is shown in the figure 4.1. The sheet charge density rises on increasing the aluminium content of the AlGaIn layer from 0.15 to 0.35. Thus, on increasing the aluminium content of the AlGaIn layer, the spontaneous and piezoelectric polarization induced charge increases in combination with the increase in conduction band offset which causes a substantial increase in the 2DEG sheet charge density in the triangular quantum well.

### 4.2 Dependence of 2DEG mobility on aluminium content with Hall measurements

The graph of 2DEG mobility as a function of aluminium content in the AlGaIn layer for the set of measurements where  $x_{Al} = 0.15, 0.23, 0.29, 0.35$  is shown in the figure 4.2. As aluminium content increases in the AlGaIn layer, the sheet charge density increases due to the increase in spontaneous and piezoelectric polarization induced charges and hence, the electrons are pushed more closely to the interface and more electrons are affected by the interface roughness scattering which ultimately limits the 2DEG mobility.

An inelastic optical phonon scattering, which is dominant at room temperature and interface roughness scattering, which is more dominant at low temperatures, also affects the mobility. At room temperature, optical phonon energies are very high and hence more electrons interact with the optical phonons which results in decreasing the mobility.

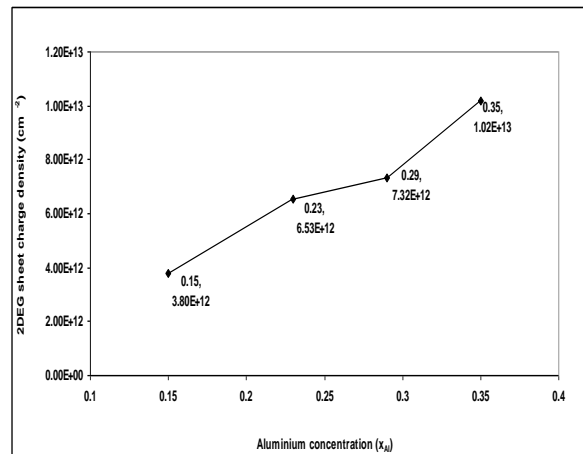


Figure 4.1: - 2DEG sheet charge density plotted as a function of aluminium concentration

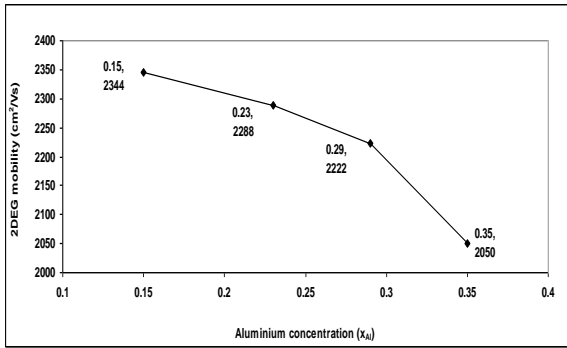


Figure 4.2: - 2DEG mobility plotted as a function of aluminium concentration

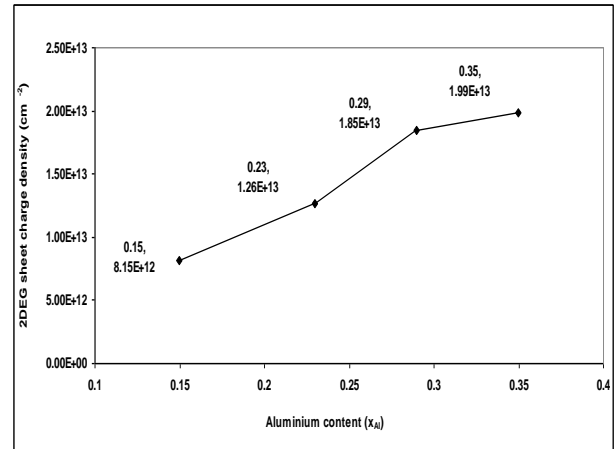


Figure 4.4: - 2DEG sheet charge density plotted as a function of aluminium concentration for 1D Poisson simulation

### 4.3 Dependence of 2DEG mobility on 2DEG sheet charge density

The graph of 2DEG mobility as a function of 2DEG sheet charge density, when aluminium content in the AlGa<sub>N</sub> layer increases from 0.15 to 0.35 is shown in the figure 4.3. The 2DEG mobility decreases on increasing the sheet charge density because, as the 2DEG sheet charge density increases on increasing the aluminium mole content because of the reason explained in the previous section, the triangular quantum well becomes narrower and hence there is strong quantum confinement in the z-direction. This strong confinement along the z-direction results in to the large number of electrons occupying the interfacial states and hence the imperfect interface at the AlGa<sub>N</sub>/Ga<sub>N</sub> Heterojunction affects the 2DEG mobility.

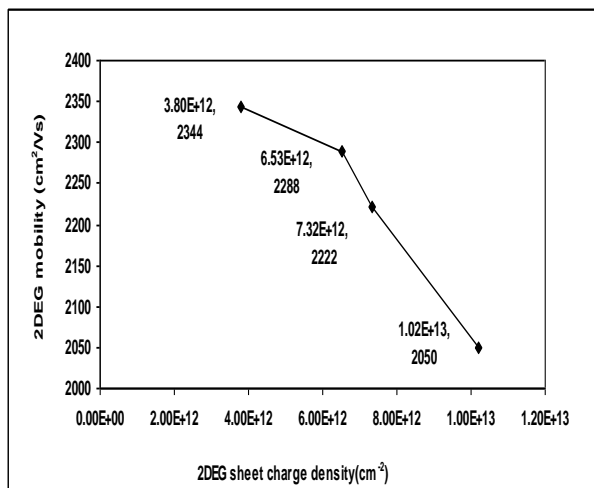


Figure 4.3: - 2DEG mobility plotted as a function of 2DEG sheet charge density

### 4.4 Dependence of 2DEG sheet charge density on aluminium content by 1D Poisson simulation

The graph of 2DEG sheet charge density as a function of aluminium content is shown in the figure 4.4. It also shows the similar result as obtained for Hall measurements. The graph shows a continuous increment in the 2DEG sheet charge density when aluminium content in the AlGa<sub>N</sub> layer is from 0.15 to 0.35. The same explanations comes here as that explained in the previous section.

### Conclusion

A field effect transistor (FET) is a very efficient device in converting a biological signal into an electrical signal due to its sensitivity to changes in the surface potential. Biosensors based on AlGa<sub>N</sub>/Ga<sub>N</sub> HEMT platforms perform very well due to the high sheet electron concentration induced by spontaneous and piezoelectric polarization and high electron mobility. The results obtained from this project are in close conjunction to that required for bio-sensing applications i.e. sheet charge density of the magnitude of  $10^{13} cm^{-2}$  and the mobility of  $2000 cm^2/Vs$ .

### Acknowledgement

I would like to thank my supervisor A/Prof. Gia Parish for guiding me through each and every aspects of this project and for being a very helpful supervisor. I would like to thank Gilberto Umana-Membrano for explaining me the theoretical and practical aspects of the project and Tamara Fehlberg for giving the thought provoking suggestions during my project.

## References

- [1]. M.S. Shur, *GaN-Based Electronic Devices, Cree research, Japan, 1998.*
- [2]. H. Morkoc, S. Strite, G.B. Gao, M.E. Lin, B. Sverdlov and M. Burns, "Large-band-gap SiC, III-V nitride, and II-VI ZnSe based semiconductor device technologies," *University of Illinois, March 1994.*
- [3]. G. Snider, *1D Poisson, University of Notre Dame, Notre Dame.*
- [4]. S. Nakamura, *The Blue laser Diode: GaN based Light Emitters and Lasers, Springer, 1997.*
- [5]. R. Gaska, J. Yang, A. Osinsky, A.D. Bykhovski and M.S. Shur, "Piezoeffect and gate current in AlGaIn/GaN High Electron Mobility Transistors," *Appl. Phys. Lett. Vol. 71, no. 25, pp. 3673, Dec. 1997.*
- [6]. S.N. Mohammad, A.A. Salvador and H. Morkoc, "Emerging Gallium Nitride Based Devices." *Proc. IEEE, vol. 83, no. 10, pp. 1306-1355, October 1995.*
- [7]. S.C. Jain, M. Willander, J.Narayan and R. Van Overstraeten, "III-nitrides: Growth, Characterisation and Properties," *J. Appl. Phys., vol. 87, no. 3, pp. 965-1006, 2000.*
- [8]. D. Steigerwald, S. Rudaz, H. Liu, R.S. Kern, W. Gotz and R. Fletcher, "III-V Nitride Semiconductors for High Performance Blue and Green Light Emitting Devices," *The Minerals, Metals & Materials Society, vol. 49, pp.18-23, 1997.*
- [9]. J. Li, B. Nam, J.Y. Lin and H.X. Jiang, "Optical and electrical properties of Al-rich AlGaIn alloys," *Appl. Phys. Lett., vol. 79, no. 20, pp. 3245-3247, Nov. 2001.*
- [10]. B.Van. Zeghbroeck, "Principles of Semiconductor Devices," 2007.
- [11]. Keithley, *Model 7065 Hall Effect Card*

## Appendix A

Calculations for the 2DEG sheet charge density obtained from 1D Poisson simulation are shown below: -  
First of all, calculations for the spontaneous and piezoelectric polarisation induced sheet charge density for all different aluminium concentration i.e.  $x = 0.15, 0.23, 0.29, 0.35$  are shown below. The piezoelectric polarisation sheet charge density is found from the following equation:-

$$P_{PE} = \frac{a - a_o}{a_o} \left( e_{31} - e_{33} \frac{C_{13}}{C_{33}} \right) \frac{C}{m^2}$$

Where,

$$\begin{aligned} a(\text{GaN}) &= 3.189 \text{ \AA}^0, \\ a_0(x) &= (-0.077x + 3.189)10^{-10} \text{ m}, \\ c_0(x) &= (-0.203x + 5.189)10^{-10} \text{ m}, \\ C_{13}(x) &= (5x+103) \text{ GPa}; \\ C_{33}(x) &= (-32x + 405) \text{ GPa}; \\ e_{31}(x) &= [e_{31}(\text{AlN}) - e_{31}(\text{GaN})]x + e_{31}(\text{GaN}) \text{ (from ref);} \\ e_{33}(x) &= [e_{33}(\text{AlN}) - e_{33}(\text{GaN})]x + e_{33}(\text{GaN}); \end{aligned}$$

The spontaneous induced sheet charge is given by:-

$$P_{SP}(x) = (-0.052x - 0.029) \frac{C}{m^2}$$

The total polarisation induced sheet charge caused by the significant change of spontaneous and piezoelectric polarisation at the AlGaIn/GaN interface is given by: -

$$\frac{\sigma}{e} (P_{SP} + P_{PE}) \text{ cm}^{-2}$$

This calculated total sheet charge is included in the 1D Poisson program as a very thin layer of  $1\text{ \AA}^0$  in the AlGaIn layer as acceptor and donor charge. The 1D program simulation gives the value of 2DEG sheet charge density.